

Hydraulic and Sediment Dynamics of the Euphrates River – Evaluating Scouring, Sediment Transport, and Riverbank Soil Characteristics at the Shatt Al-Hilla Reach

Zaid Gaber Ghaib^{1*}, Kareem R. Al-Murshedi¹, Ahmed Samir Naje¹

¹ Department of Water Resources Management Engineering, College of Engineering, Al-Qasim Green University, Babylon 51013, Iraq

* Corresponding author's e-mail: zaydjaber1@gmail.com

ABSTRACT

This study aims to investigate sediment dynamics and scouring processes in the Shatt Al-Hilla reach of the Euphrates River, with a focus on the hydraulic characteristics and soil properties influencing meandering behavior and erosion susceptibility. Bed material samples were collected from 20 river sections to assess sediment characteristics. Laboratory analyses included specific gravity measurements, grain size distribution, and soil classification using the Unified Soil Classification System (USCS). Specific gravity values ranged from 2.61 to 2.77, and grain size analysis revealed d_{50} values between 0.166 mm and 0.339 mm. Soil classification identified a range of poorly graded sands (SP) and well-graded sands with silt (SW-SM). The study finds significant variability in sediment characteristics across the river sections. Sections with higher specific gravity and well-graded sediments show greater stability, while those with lower specific gravity and poorly graded sands are more prone to erosion and scouring. This variability affects bed stability and sediment transport dynamics. The results highlight that sediment composition and gradation play critical roles in scouring processes and riverbank stability. The study is limited to the specific reach of the Euphrates River and may not be generalizable to other river systems without similar sediment analyses. The findings emphasize the need for detailed sediment characterization in river management but do not address the long-term impacts of sediment dynamics on river morphology. Understanding sediment variability and its impact on scouring processes can aid in predicting erosion patterns and designing more effective river management practices tailored to specific sediment characteristics. This research provides novel insights into the relationship between sediment properties and scouring behavior in the Al-Hilla reach, filling gaps in the understanding of sediment dynamics in meandering rivers. The detailed analysis of sediment characteristics and their influence on river stability offers new perspectives for future research and practical applications in river management.

Keywords: sediment dynamics, scouring processes, grain size distribution, hydraulic characteristics, riverbank soil properties, stream restoration.

INTRODUCTION

Rivers are vital geomorphic and ecological systems that shape landscapes and sustain diverse ecosystems. However, processes such as erosion, sedimentation, and meandering, while fundamental to their natural dynamics, can create significant challenges for human infrastructure and settlements (Frasson et al., 2019; Ghadampour et al., 2020). The Shatt Al-Hilla reach of the Euphrates River exemplifies these challenges, exhibiting

complex hydraulic conditions and diverse sediment properties that contribute to ongoing issues of riverbank erosion and sedimentation (Giovanni, 2006; Alfatlawi and Alsultani, 2019).

The Shatt Al-Hilla reach is particularly prone to severe meandering and sedimentation issues, largely driven by its unique sediment dynamics and hydraulic conditions (Harrelson, 1994; Salahaldain et al., 2023). Recent studies have noted that meandering behavior in rivers is influenced by various factors, including flow velocity,

discharge variability, and sediment load (Kuntjoro et al., 2017; Ikhsan et al., 2019). However, specific research on the interplay between sediment characteristics and hydraulic conditions at localized river segments like Shatt Al-Hilla remains limited.

Prior research has indicated that sediment properties such as grain size distribution and specific gravity significantly impact riverbank stability and sediment transport (Sinnakaudan et al., 2010; Alfatlawi and Alsultani, 2018a). For instance, (WRDS, 2018) found that variations in sediment grain size could lead to differential erosion rates along riverbanks, yet detailed studies integrating sediment density and hydraulic parameters are lacking. The influence of sediment gradation on meandering patterns and erosion dynamics remains poorly understood, particularly in regions with complex sedimentary environments (Bowels, 1970).

This study addresses these research gaps by investigating the sediment dynamics and hydraulic characteristics specific to the Shatt Al-Hilla reach. The hypothesis posited is that variations in sediment properties, including specific gravity and grain size distribution, play a critical role in influencing meandering behavior and erosion rates. Specifically, it is anticipated that areas with higher specific gravity and well-graded sediments will exhibit greater stability compared to sections with lower specific gravity and poorly graded sediments (Alsultani et al., 2023a). This hypothesis is informed by preliminary observations and previous findings that suggest sediment characteristics are pivotal in shaping river dynamics (Brockman, 2010).

The Shatt Al-Hilla reach's susceptibility to severe meandering and sedimentation underscores the need for a detailed understanding of sediment-hydraulic interactions. The unique sediment dynamics and hydraulic conditions in this region create a context-specific scenario that has not been thoroughly explored in previous studies (Dakheel et al., 2022). By providing a detailed analysis of sediment characteristics and hydraulic parameters, this research aims to enhance predictive models for river management and offer targeted strategies for mitigating erosion and sedimentation impacts.

This study makes a novel contribution by combining detailed sediment analyses with hydraulic modeling tailored to the Shatt Al-Hilla reach. Previous research has often addressed

broader trends in river dynamics without focusing on localized sediment-hydraulic interactions (Thair et al., 2018). By filling this gap, the study offers new insights into how specific sediment properties influence river behavior, thereby improving the understanding of river dynamics and informing more effective river management and restoration strategies.

METHODOLOGY

Due to the absence of direct studies focusing on the hydraulic geometry relationships in the Shatt Al-Hilla region, this research aims to evaluate and validate universal hydraulic relationships within this context (Dash and Khatua, 2013). Subsequently, the study endeavors to develop new, more suitable relationships tailored to control the meandering processes along the Shatt Al-Hilla reach (Eaton et al., 2010; Alsultani and Khassaf, 2022; Forti et al., 2023). To achieve these objectives, a comprehensive work program was designed, consisting of both field and laboratory work. The fieldwork was conducted over the period from January 2023 to December 2023.

Case study selected

This section describes the Shatt Al-Hilla River and details the data collected from the study area, including geological, climatic, hydrological, and location-specific information. These data points are crucial for understanding factors that directly or indirectly impact the study (Griffiths, 1980; Frasson et al., 2019; Alsultani et al., 2022a).

The Shatt Al-Hilla River flows through the center of Al-Hillah in Babylon Province, Iraq, with coordinates 32°3'16" N and 44°46'29" E. As the largest branch of the Euphrates River, it stretches 100 km from Babylon Province to Diwaniyah Governorate. The river draws its water from the left bank of the Euphrates, just upstream of the New Hindiya Barrage, irrigating extensive agricultural lands and the center of Hilla city, while also recharging the shallow groundwater system within the studied area at varying rates (Alsultani et al., 2022b).

The river serves as a vital water source for nearby cities. During operation, the flow rate varies significantly, from 230 m³/s at the Al-Hillah Head Regulator to 45 m³/s at the Shatt Al-Hillah Regulator (Maarroof and Kareem, 2022). The

study area covers the reach downstream of the Al-Hillah Regulator to upstream of the Al-Saadda Regulator, as illustrated in Figure 1.

The Shatt Al-Hilla lies within the Mesopotamian plain on the unstable shelf, also known as the Mesopotamian zone within the Geosyncline Basin, situated between the Zagros Mountains in the northeast and the stable Arabian plateau in the southwest (Alfatiawi et al., 2020). The region is predominantly covered with Quaternary sediments from the Pleistocene and Holocene epochs, characterized by floodplain deposits from the Euphrates River and its branches. The area is also influenced by regional tectonic movements, which have created a symmetric concave fold in the sedimentary plain, continuously filled with river sediments, in addition to deposits from branches and depression fill deposits produced by floods, mainly composed of fine sand, clay, silt, and silty clay (Maarouf and Kareem, 2022).

Climate of the region

The Shatt Al-Hilla flows through a uniform climatic zone characterized by hot, dry summers and cold, wet winters. The region receives sparse rainfall, averaging 75 mm annually in Al-Hillah city, with most precipitation occurring during the winter months (McCandless, 2003). The average annual precipitation in the study area is 80 mm, with maximum rainfall typically occurring in January and February, and no precipitation during July

and August. Summers are particularly harsh, with daytime temperatures reaching up to 50 °C, while the average temperature is 24 °C (GAGW, General Authority for Groundwater in Al-Hillah city).

Geology of the region

The geology of the study area is dominated by the following formations (Alfatlawi and Alsultani, 2018b):

- Al-Sadda Deposits: located on both sides of the Euphrates River;
- Al-Hilla Formation: composed of pebbly sandstone;
- Al-Hashimiyah Formation: a cap rock over the Al-Hilla formation, formed by capillary action due to underground water oscillations, containing secondary gypsum and sandstone, as presented in Figure 2.

Hydrology of the region

The annual average inflow of the Shatt Al-Hilla River, until 1989, was 27.4 BCM. However, from 1989 to 2012, the average annual flow decreased to 17.4 BCM due to climatic conditions and the construction of upstream dams. This variability in water inflows has caused fluctuations in high, low, and dry periods throughout the year, with the minimum recorded inflows being 9.02 BCM in 1974 during the impoundment of the Syrian and Turkish dams of Tabaqa and Keban (Nanson et al., 2010).



Figure 1. Location of the selected study area

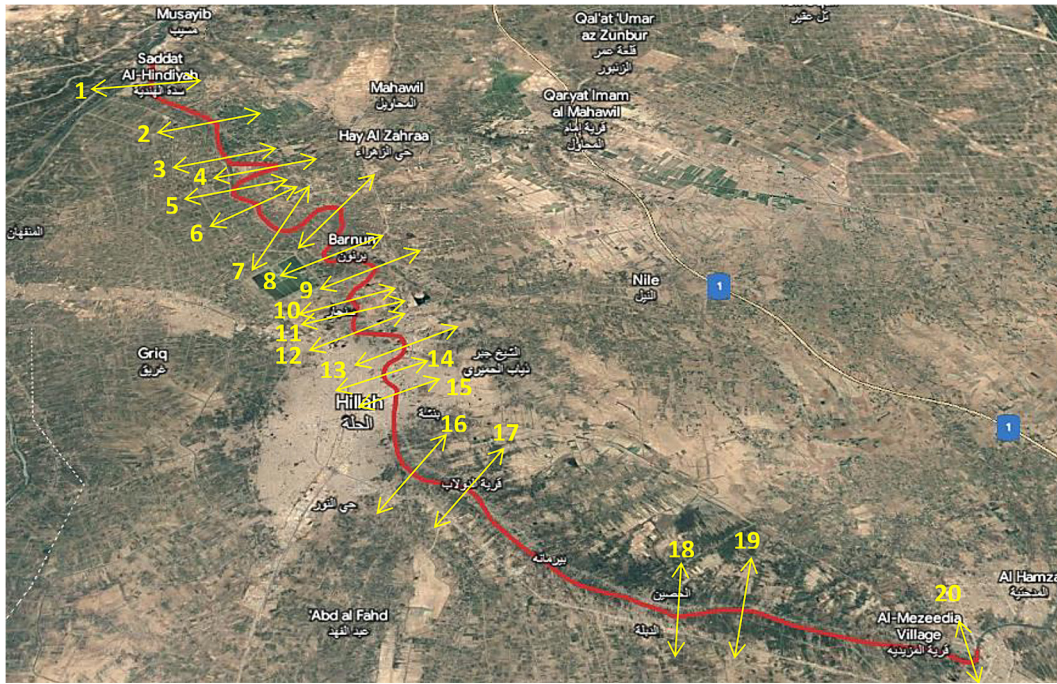


Figure 2. Geology of the Shatt Al-Hilla

Zone selection

This research examines the effects of the Shatt Al-Hilla River’s characteristics on the meandering process. The study area covers a 51.1 km reach between Saddat Al-Hindiyyah (32°43’41”N, 44°16’10”E) and Al-Hashimiyah city (32°22’29”N, 44°39’06”E), as depicted in Figure 3.

Field work

This section outlines the phases of fieldwork, which involved collecting and measuring the hydraulic characteristics of river sections, determining the longitudinal slopes of the stream, and soil sampling. The tools and equipment used in these processes are also described. Most cross-sectional

data were measured using an Acoustic Doppler Current Profiler (ADCP). Longitudinal surveys were conducted using a level with tripod, level rod, tapes, pins, and a laptop to log data. For bed material analysis, standard equipment such as cans, tubes, and cutters were used. Additional equipment, including a computer, internet, software, GPS, and GIS techniques, were utilized to collect and analyze the meandering characteristics (Alsultani et al., 2023b).

The ADCP is used to measure water velocity and profiles by sending sound waves across the river’s cross-section, which collide with particles in the bed. The device calculates the difference between the frequencies emitted and received, representing the speed of water flow in the river. Certain procedures must be followed

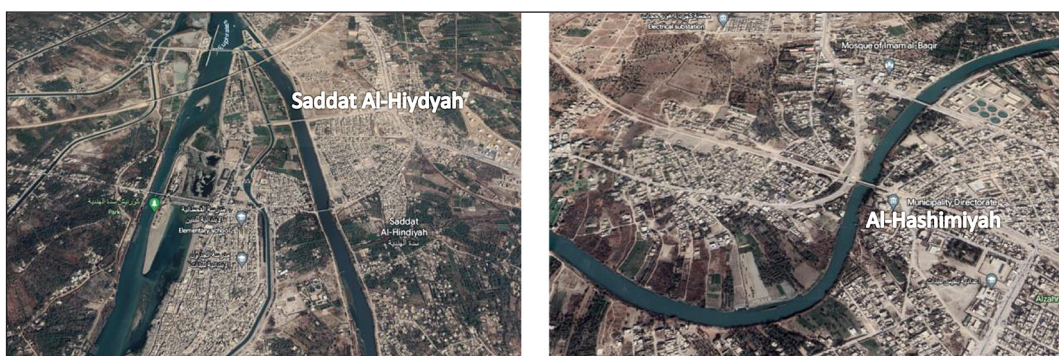


Figure 3. Location of the selected reach (Google Earth)

before measurements using the ADCP to ensure accurate results, such as compass calibration, system checks, and inputting values for salinity and magnetic declination. Local slopes were measured following the methods outlined by (Odemerho, 1984).

Main channel slopes were computed for each surveyed section using Google Earth, with the average slope calculated as the difference in elevation divided by the distance between points (Odemerho, 1984). The study area was divided into 20 stations representing key meandering points along the Al-Hilla River. Table 1 lists the coordinates and distances of the selected sections. Twenty boreholes were drilled, with a depth of 10 m at each station.

At least one sample was collected from each of the 20 sections in the reach. Particle size distribution graphs were produced, and the median particle size (d_{50}) for each sample was determined. Soil classification was conducted according to the Unified Soil Classification System (USCS).

Laboratory measurements

The laboratory work included tests for mechanical and physical properties, conducted at the Construction Laboratories of Babylon. Test scenarios

varied depending on the sample type: Disturbed Samples (DS), Split Spoon (SS), and Undisturbed Samples (US), following ASTM standards.

The physical properties tests included:

1. Grain size distribution: ASTM (422) – sieving and sedimentation processes.
2. Moisture content test: ASTM (2488) – visual classification of soil properties.
3. Specific gravity test: ASTM (854) – determination of specific gravity using a water pycnometer.
4. Atterberg limits test: ASTM (4318) – classification of soils based on moisture content.
5. Unit weight test: ASTM (4318) – determination of wet and dry unit weights.

The mechanical properties tests included:

1. Consolidation test: ASTM (2435-02) – measurement of soil compression under controlled conditions.
2. Direct shear test: ASTM (D3080-04) – Measurement of shear resistance of soils.

Measurements of hydraulic geometry

Hydraulic geometry relationships (HG) were assessed for the Shatt Al-Hilla River based on

Table 1. Coordinates and distances of selected sections on Shatt Al-Hilla

Station No.	Latitude line (°)	Longitude line (°)	Outer Bank length (m)	Inner Bank length (m)
1	32.41.27	44.16.51	212	204
2	32.40.04	44.19.21	271	258
3	32.39.57	44.20.02	347	346
4	32.38.02	44.21.50	200	198
5	32.36.41	44.20.34	167	110
6	32.36.10	44.21.27	118	97
7	32.34.46	44.22.27	70	50
8	32.36.03	44.23.59	193	152
9	32.33.56	44.23.44	171	147
10	32.33.28	44.25.22	137	99
11	32.32.17	44.24.41	216	150
12	32.31.05	44.25.00	117	93
13	32.30.40	44.26.21	204	192
14	32.29.44	44.26.54	107	96
15	32.29.13	44.26.21	286	215
16	32.26.59	44.26.42	197	193
17	32.26.23	44.28.09	214	208
18	32.23.12	44.34.54	205	194
19	32.23.20	44.34.24	165	148
20	32.22.10	44.38.54	134	115

data from 20 stations along the reach. Measurements included channel width, depth, and water surface slope, which were analyzed to evaluate the HG exponents and coefficients.

This section describes the process for determining hydraulic characteristics and the geometry of the river. It also includes a detailed description of the field and laboratory methods used to gather data and how these data were analyzed to determine the HG relationships for the Shatt Al-Hilla reach. The ultimate goal is to develop site-specific relationships to predict river behavior, including meandering processes.

RESULTS AND DISCUSSION

This section provides an overview of the results obtained from various measurements, both in the field and in the laboratory, which will be

analyzed to establish hydraulic geometry relationships for the Shatt Al-Hilla River.

Climate outcomes

The climate data for Al-Hilla city was collected from the Babylon climate station, covering the period from 1980 to 2023. The data includes temperature and rainfall, with results summarized in Tables 2 and 3, and visually represented in Figure 4. The climate diagram shows the variations in temperature and rainfall, highlighting the seasonal changes that might influence the river’s hydraulic characteristics.

Hydrology of the region

The hydrology of the Euphrates River at Al-Hilla is characterized by three distinct flow regimes:

Table 2. Average monthly temperature in Al-Hilla city

Month	Min. Temp. C°	Max. Temp. C°
Jan.	5.2	16
Feb.	7	19.9
Mar.	11.1	23.7
April	16.9	30.6
May	22.5	37.1
June	26.3	41.7
July	28.6	44
Aug.	27.5	43.5
Sep.	24.2	40.3
Oct.	18.6	33.4
Nov.	11.8	24.2
Dec.	6.5	17.9

Table 3. Average monthly rainfall in Al-Hilla in (mm)

Month	Average monthly rainfall (mm)
Jan.	19.8
Feb.	16.9
Mar.	15.4
April	12.2
May	4.6
June	0.04
July	-
Aug.	-
Sep.	0.04
Oct.	4.3
Nov.	13.5
Dec.	15.4

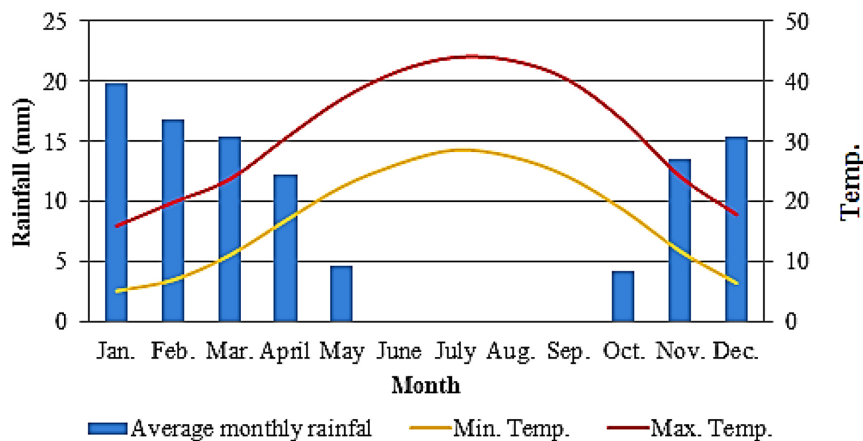


Figure 4. Climate diagram for the selected river reach

- high flows: occur between February and June, accounting for approximately 75% of the annual flow;
- low flows: occur between July and October, representing about 10% of the annual flow;
- moderate flows: occur between November and February, contributing about 15% of the annual flow.

The analysis of flow data from 2000–2017 shows a declining trend in the annual flow of the Euphrates River, with only a few years exceeding

the historical average flow. The development of water resources, particularly the GAP projects in Turkey, is expected to reduce inflow and affect water quality. Figure 5 presents the average annual flow of the river for the period 2000–2017.

Results of the field work

This section presents the data collected from the field measurements, including the dimensions of the selected river reach, cross-sections, water discharge, and longitudinal slopes.

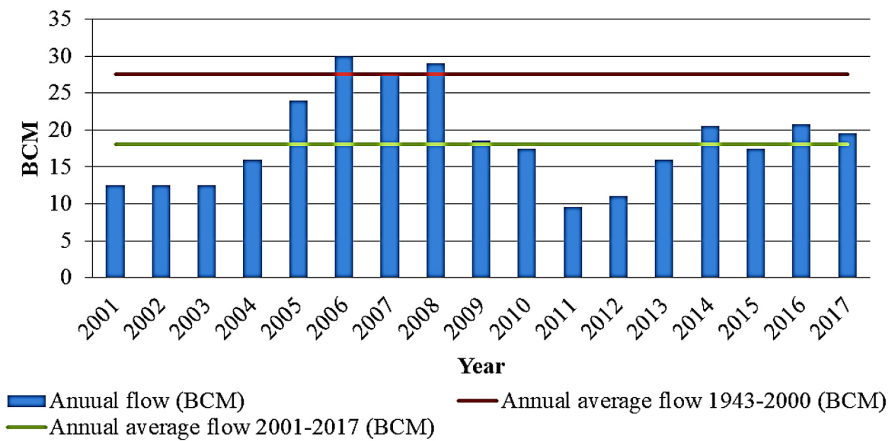


Figure 5. The average annual flow of the river for period 2001–2017

Table 4. Discharge values in each section

Section no.	Discharge(Q) m ³ /sec	Section No.	Discharge(Q) m ³ /sec	Section No.	Discharge(Q) m ³ /sec
1	65.45	8	35.35	15	78.64
2	63.12	9	33.86	16	74.08
3	66.33	10	52.35	17	58.65
4	56.75	11	53.19	18	57.35
5	41.62	12	47.46	19	52.57
6	33.41	13	62.04	20	34.43
7	37.75	14	68.72		

Table 5. Width values in each section

Section no.	Width (w) m	Section no.	Width (w) m	Section no.	Width (W) m
1	111.92	8	53.78	15	184.12
2	107.91	9	48.01	16	140.48
3	112.02	10	82.12	17	96.55
4	93.78	11	83.9	18	97.24
5	62.19	12	71.92	19	84.22
6	47.81	13	103.02	20	49.46
7	56.05	14	115.77		

Cross-sections and water discharge

The cross-sectional survey involved detailed measurements at various locations along the river to capture the hydraulic properties of different river sections. Tables 4 to 9 present the results, including discharge, width, mean depth, area, mean velocity, and maximum depth at each section. Stations with high curvature, such as stations 7 and 14, exhibited higher velocities. Figures 6 and 7 illustrate measurements taken by the ADCP device at sections 7 and 10.

Main slopes outcomes

The slope analysis was conducted using both Google Earth and field data, with results summarized in Table 10 and Figure 8 compare the main

slopes obtained from Google Earth and fieldwork. The findings show that slope varies significantly between sections, with narrower sections exhibiting steeper slopes

Laboratory measurements

This section presents the results of laboratory analyses conducted on bed material samples collected from the river.

Specific gravity

The specific gravity values of the bed material ranged from 2.61 to 2.77 across the different sections of the river, as shown in Table 11. These values suggest variations in the mineral

Table 6. Mean depth values in each section

Section no.	Mean depth (dm) (m)	Section no.	Mean depth (dm) (m)	Section no.	Mean depth (dm) (m)
1	1.48	8	3.46	15	1.66
2	1.79	9	3.8	16	2.12
3	1.76	10	2.83	17	2.64
4	2.27	11	4	18	2.45
5	3.13	12	3.06	19	2.65
6	4.53	13	2.89	20	3.79
7	3.34	14	2.29		

Table 7. Area estimation in each section

Section no.	Area (a) (m ²)	Section no.	Area (a) (m ²)	Section no.	Area (A) (m ²)
1	213	8	305	15	297.1
2	248.9	9	215.6	16	293.6
3	152.3	10	251.2	17	539
4	404.6	11	206.7	18	251.5
5	194	12	245.1	19	239.1
6	210.5	13	260.9	20	205
7	133.2	14	249.7		

Table 8. Mean velocity values in each section

Section no.	Mean velocity (v) (m/sec)	Section no.	Mean velocity (v) (m/sec)	Section no.	Mean velocity (v) (m/sec)
1	0.31	8	0.12	15	0.27
2	0.25	9	0.16	16	0.25
3	0.43	10	0.21	17	0.11
4	0.14	11	0.26	18	0.23
5	0.22	12	0.19	19	0.22
6	0.16	13	0.24	20	0.17
7	0.28	14	0.28		

Table 9. Max. depth values in each section

Section no.	Maximum depth (dmax) (m)	Section no.	Maximum depth (dmax) (m)	Section no.	Maximum depth (dmax) (m)
1	3	8	4.4	15	2.8
2	3.1	9	9	16	3
3	2.3	10	4.6	17	3.7
4	3	11	7.9	18	3.3
5	7.8	12	5.3	19	5.3
6	7.5	13	3.7	20	6.7
7	6.1	14	2.9		

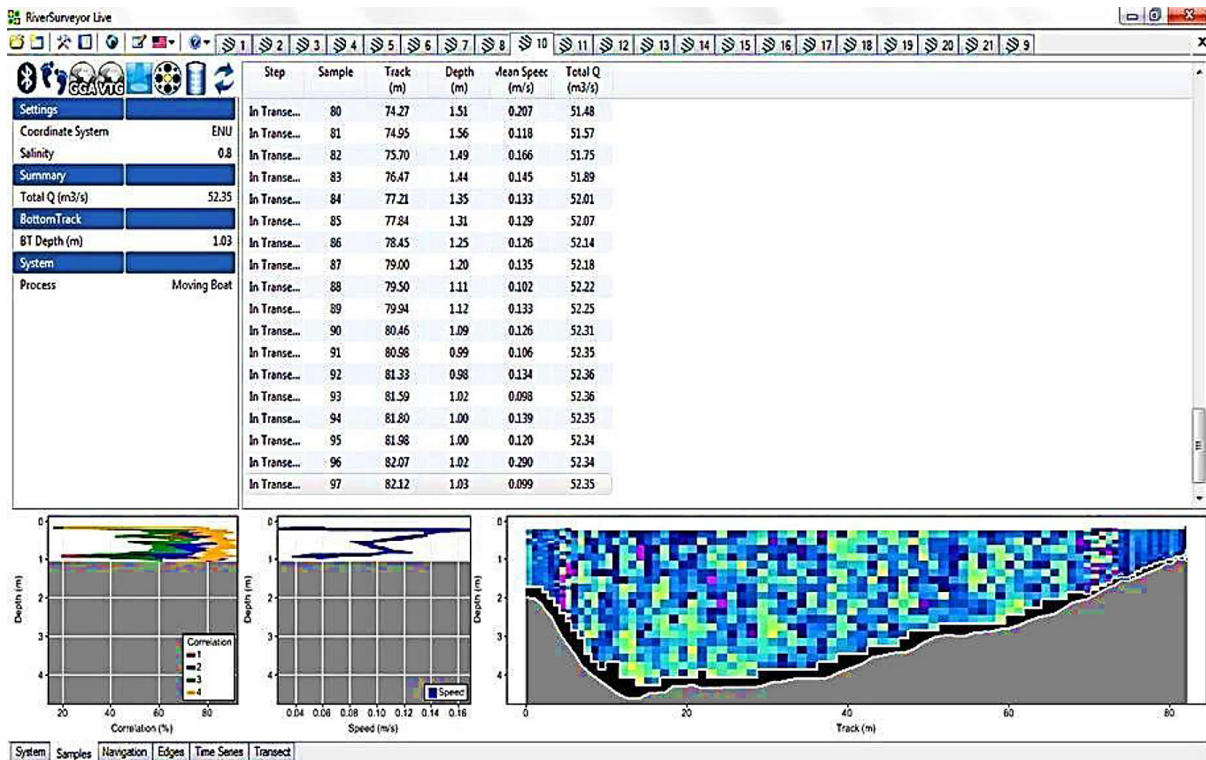


Figure 6. Measurement by ADCP in section No.7

composition and density of the sediments in different parts of the river. Higher specific gravity values (e.g., 2.77 in Section 9) indicate the presence of denser minerals, possibly including quartz, feldspar, or heavy minerals like magnetite. Conversely, lower values (e.g., 2.61 in Section 15) could suggest a higher proportion of lighter minerals or organic content. These variations in specific gravity are crucial for understanding the behavior of sediment clusters. Higher specific gravity sediments are more prone to settling quickly, leading to coarser sediment deposits in areas of the river with slower flow rates. In contrast, lower specific gravity sediments may

be transported further downstream before settling, contributing to finer sediment deposits in areas with higher flow velocity. The range of specific gravity values implies that sediment transport processes will vary significantly along the river. Sections with higher specific gravity values are likely to experience more pronounced deposition of coarser sediments, potentially leading to changes in riverbed morphology, such as the formation of gravel bars. On the other hand, sections with lower specific gravity values may have finer sediments that are more easily resuspended, leading to greater sediment transport and potential scouring during high-flow events.

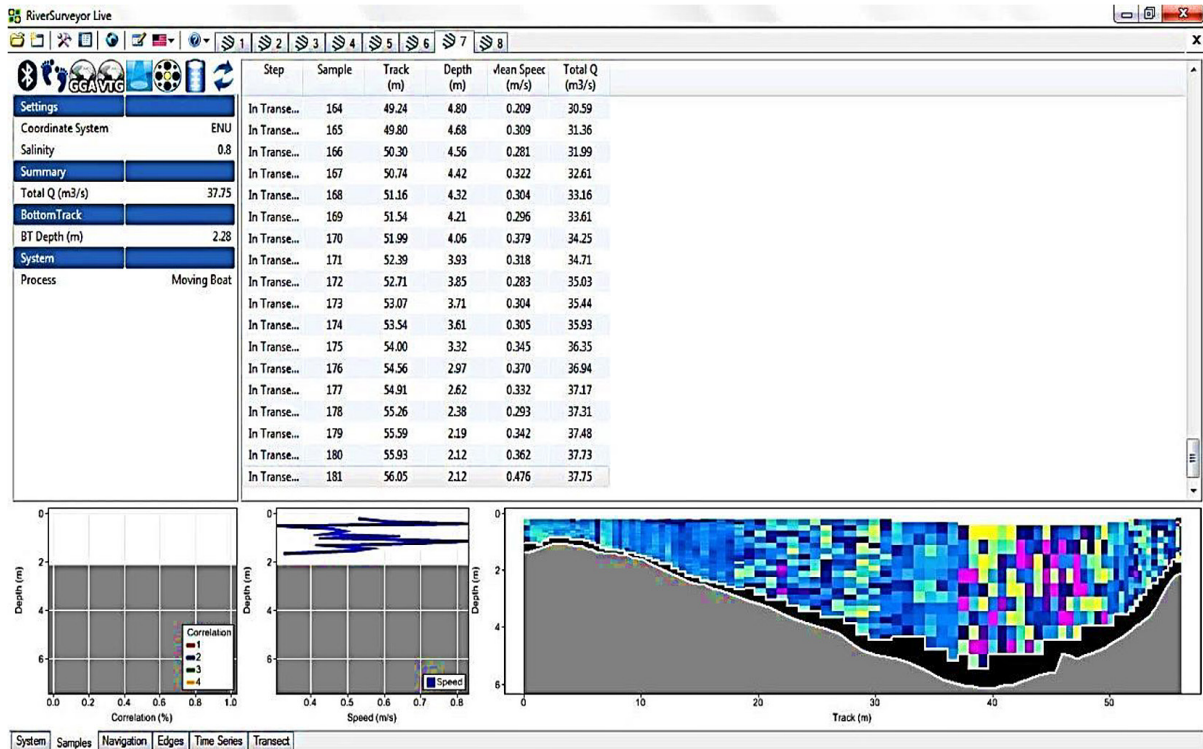


Figure 7. Measurement by ADCP in section No. 10

Table 10. Main slope values for reach sections

Section No.	Main Slope	Section No.	Main Slope	Section No.	Main Slope
1	0.00055	8	0.00220	15	0.00116
2	0.00002	9	0.00831	16	0.00109
3	0.00120	10	0.00645	17	0.00038
4	0.00356	11	0.00895	18	0.00087
5	0.01085	12	0.00060	19	0.00606
6	0.02000	13	0.00581	20	0.00929
7	0.00069	14	0.00142		

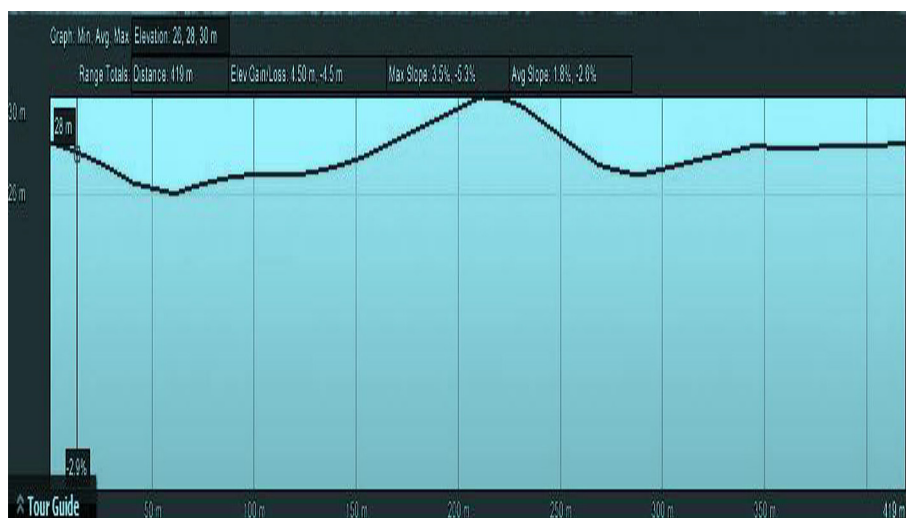


Figure 8. Main slope by (Google Earth)

Table 11. Specific gravity values at each section

Section no.	Specific gravity (gs)	Section no.	Specific gravity (gs)	Section no.	Specific gravity (gs)
1	2.64	8	2.75	15	2.61
2	2.63	9	2.77	16	2.62
3	2.63	10	2.71	17	2.66
4	2.67	11	2.69	18	2.68
5	2.73	12	2.74	19	2.67
6	2.77	13	2.65	20	2.76
7	2.75	14	2.63		

Grain size analysis of bed materials

Grain size analysis is a fundamental aspect of sedimentology, providing insights into the texture, sorting, and sediment transport mechanisms in the river. The mean size (d50) values, shown in Table 12, and the grain size distribution curves, presented in Figures 9 and 10, offer a detailed understanding of the sediment composition across different sections.

The grain size distribution varies across the sections, with d50 values ranging from 0.166 mm

(Section 6) to 0.339 mm (Section 15). These values indicate that the sediments are predominantly in the sand to sandy silt range, with some sections exhibiting finer or coarser materials.

The grain size distribution curves for Sections 1–10 and 11–20 highlight the variability in sediment sizes, which can be attributed to differences in hydraulic conditions, sediment supply, and riverbed morphology. Sections with finer sediments (e.g., Sections 6 and 8) are likely to be located in areas with lower energy conditions, where fine particles can settle.

Table 12. Mean size values for each section

Section no.	D50 (mm)	Section no.	D50 (mm)	Section no.	d50 (mm)
1	0.263	8	0.187	15	0.339
2	0.249	9	0.173	16	0.325
3	0.267	10	0.214	17	0.23
4	0.225	11	0.222	18	0.229
5	0.189	12	0.199	19	0.218
6	0.166	13	0.237	20	0.186
7	0.188	14	0.269		

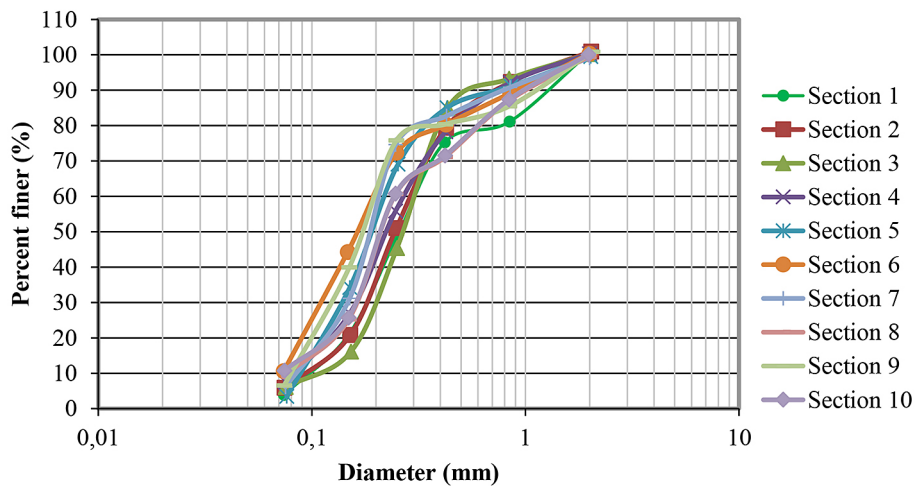


Figure 9. Grain size distribution curve for section (1–10)

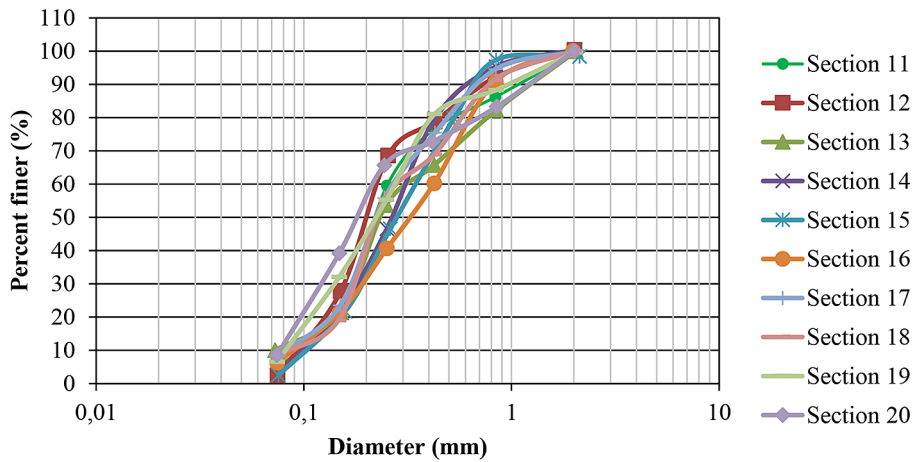


Figure 10. Grain size distribution curve for Section (11–20)

In contrast, sections with coarser sediments (e.g., Sections 15 and 16) may be in higher energy areas where only larger particles can settle. The results demonstrated that, as indicated in Table 13, the sediment type of beds load transfers are sand badly to highly graded as well as sandy silt in certain stations. The bed load transporters’ average diameter values (D50) range widely from 0.1 mm to 1.2 mm.

The discharge values have an impact on the bed load transport values, which vary widely. The outcomes of results are consistent with previous studies (Xiaoqing and Yang, 2003; Ollero, 2010; Hasan et al., 2024). Table 13 classifies the soil according to the Unified Soil Classification System (USCS), with classifications ranging from poorly graded sand (SP) to well-graded sand with silt (SW-SM). Poorly graded sands (e.g., Sections 1, 5, 11) suggest a uniform grain size distribution, which can result in higher porosity and permeability. These sections are more susceptible to erosion and scouring, particularly during high-flow events.

Well-graded sands with silt (SW-SM), found in several sections (e.g., Sections 2, 3, 9), indicate a wider range of grain sizes, leading to better

compaction and lower permeability. These sections are likely more stable and less prone to erosion, providing a more resilient riverbed structure.

The grain size analysis and soil classification results have significant implications for sediment transport dynamics and river management. The variation in grain size and soil classification across the sections suggests that different parts of the river will respond differently to hydraulic forces. Sections with finer, poorly graded sands may experience higher rates of sediment transport and deposition, leading to potential issues with sediment accumulation and channel instability.

In contrast, sections with well-graded sands may be more stable, but they could also contribute to sediment starvation downstream if sediment transport is limited. Understanding these dynamics is crucial for developing effective river management strategies, including dredging, sediment trapping, and bank stabilization measures.

The findings in this study are consistent with previous research, which also observed significant variability in sediment characteristics and their impact on sediment transport and river morphology. The alignment of results with these

Table 13. Classification of soil according to USCS in each section

Section No.	Soil classification	Section No.	Soil classification	Section No.	Soil classification
1	(SP)	8	(SW-SM)	15	(SP)
2	(SW-SM)	9	(SW-SM)	16	(SW-SM)
3	(SW-SM)	10	(SW-SM)	17	(SW-SM)
4	(SW-SM)	11	(SP)	18	(SW-SM)
5	(SP)	12	(SP)	19	(SW-SM)
6	(SW-SM)	13	(SW-SM)	20	(SW-SM)
7	(SW-SM)	14	(SP)		

studies enhances the reliability of the findings and provides a solid foundation for future research and river management practices.

The laboratory analysis of bed material samples provides a detailed understanding of the sediment characteristics in the river, highlighting significant variability in specific gravity, grain size distribution, and soil classification across different sections. These findings are critical for understanding sediment transport processes, riverbed stability, and scouring risks. The results underscore the need for targeted river management strategies that consider the unique sediment dynamics in each section of the river.

CONCLUSIONS

This study investigated the hydraulic dynamics and sediment transport in the Euphrates River at the Shatt Al-Hilla reach. Key findings include:

1. The river exhibits high flows from February to June, low flows from July to October, and moderate flows from November to February. Discharge rates and velocities vary significantly, influenced by river dimensions and meandering.
2. Bed sediments vary from well-graded sands to sandy silts, with specific gravities between 2.61 and 2.77. Median grain sizes (d_{50}) range from 0.166 mm to 0.339 mm, affecting sediment transport behaviors.
3. Riverbank soils, classified as sandy and silty, impact erosion and stabilization efforts.
4. High curvature meanders significantly influence sediment deposition and erosion patterns. The study observed pronounced sediment accumulation in areas with sharp bends, affecting overall sediment load distribution.
5. The presence of vegetation along the riverbanks appears to mitigate erosion and sediment movement, highlighting the importance of riparian vegetation in river management.
6. Historical climate data show that variations in rainfall and temperature patterns have a substantial impact on river flow regimes and sediment transport. Climate change could further exacerbate these impacts, emphasizing the need for adaptive management strategies.

Future research should focus on long-term monitoring to refine sediment transport and hydraulic models, and assess the impact of climate

change on river dynamics. Investigating the role of riparian vegetation in erosion control and advancing sediment transport models are crucial for accurate predictions and effective management. Additionally, evaluating sediment management practices and adopting integrated river management approaches will be essential for sustainable river health and resilience.

REFERENCES

1. Alfatlawi, T.J.M. and Alsultani, R.A.A., 2018a. Determination of the degree of saturation and chloride penetration in cracked hydraulic concrete structures: Using Developed Electrical Conductivity Technique. *Indian Journal of Science and Technology*, 11, 37.
2. Alfatlawi, T.J., Alsultani, R.A., 2018b. Numerical modeling for long term behavior of chloride penetration in hydraulic concrete structures. *Global Scientific Journal of Civil Engineering*, 1.
3. Alfatlawi, T.J., Mansori, N., Alsultani, A., 2020. Stability Assessment of diaphragm cellular cofferdams subjected to severe hydro-structural conditions. *Open Civil Engineering Journal*, 14(1), 44–55.
4. Alfatlawi, T.J. and Alsultani, R.A., 2019. Characterization of chloride penetration in hydraulic concrete structures exposed to different heads of seawater: Using hydraulic pressure tank. *Engineering Science and Technology, an International Journal*, 22(3), 939–946. <https://doi.org/10.1016/j.jestech.2019.02.001>
5. Alsultani, R., Karim, I.R., Khassaf, S.I., 2022a. Dynamic response of deepwater pile foundation bridge piers under current-wave and earthquake excitation. *Engineering and Technology Journal*, 40(11), 1589–1604. <https://doi.org/10.30684/etj.2022.135776.1285>
6. Alsultani, R., Karim, I.R., Khassaf, S.I., 2022b. Mathematical formulation using experimental study of hydrodynamic forces acting on substructures of coastal pile foundation bridges during earthquakes: As a model of human bridge protective. *resmilitaris*, 12(2), 6802–6821.
7. Alsultani, R.A.A., Salahaldain, Z., Naimi, S., 2023a. Features of monthly precipitation data over Iraq obtained by TRMM Satellite for sustainability purposes. *Journal homepage: http://ajses.uomus.edu.iq*, 1(2), 1–16.
8. Alsultani, R. and Khassaf, S.I., 2022. Nonlinear dynamic response analysis of coastal pile foundation bridge pier subjected to current, wave and earthquake actions: As a model of civilian live. *resmilitaris*, 12(2), 6133–6148.
9. Alsultani, R., Karim, I.R., Khassaf, S.I., 2023b.

- Dynamic response analysis of coastal piled bridge pier subjected to current, wave and earthquake actions with different structure orientations. *International Journal of Concrete Structures and Materials*, 17(1), 1–5. <https://doi.org/10.1186/s40069-022-00561-5>
10. Bowels, J.E., 1970. *Engineering properties of soils and their measurement*. New York: McGraw Hill-Book Company.
 11. Brockman, R.R., 2010. *Hydraulic geometry relationships and regional curves for the inner and outer bluegrass regions of Kentucky*. Doctoral dissertation, University of Kentucky Libraries.
 12. Dakheel, A., Al-Aboodi, A., Abbas, S., 2022. Assessment of annual sediment load using mike 21 model in Khour Al-Zubair Port, South of Iraq. *Basrah Journal of Engineering Sciences*, 22, 108–114.
 13. Dash, S., Khatua, K., 2013. Energy loss for a highly meandering open channel flow. *Research Journal of Engineering Sciences*, 2(4), 22–27.
 14. Eaton, B.C., Millar, R.G. Davidson, S., 2010. Channel patterns: Braided, anabranching, and single-thread. *Geomorphology*, 120(3–4), 353–364.
 15. Frasson, R.P.D.M., Pavelsky, T.M., Fonstad, M.A., Durand, M.T., Allen, G.H., Schumann, G., Lion, C., Beighley, R.E., Yang, X., 2019. Global relationships between river width, slope, catchment area, meander wavelength, sinuosity, and discharge. *Geophysical Research Letters*, 46(6), 3252–3262.
 16. Frasson, R.P., Ferro, V., Rinaldi, M., 2019. The effect of river channel geometry on the hydraulic behavior of meandering rivers: Insights from a comprehensive data analysis. *Journal of Hydrology*, 570, 245–260. <https://doi.org/10.1016/j.jhydrol.2019.01.038>
 17. Giovanni, A., 2006. Sediment transport and deposition in river meanders: Case studies and model evaluations. *Geomorphology*, 74(1–4), 243–254. <https://doi.org/10.1016/j.geomorph.2005.08.001>
 18. Ghadampour, A., Moghimi, H., Tavakoli, H., 2020. Impact of meander belt width on average river discharge and velocity: A study of the river transit dynamics. *Water Resources Research*, 56(3), 214–229. <https://doi.org/10.1029/2019WR026036>
 19. Griffiths, G.A., 1980. Hydraulic geometry relationships of some New Zealand gravel bed rivers. *Journal of Hydrology (New Zealand)*, 106–118.
 20. Harrelson, C.C., 1994. *Stream channel reference sites: An overview of the process of developing reference sites*. USDA Forest Service Technical Report. Available at: <https://www.fs.usda.gov/treesearch/pubs/6738>
 21. Hasan, R.F., Seyedi, M., Alsultani, R., 2024. Assessment of Haditha Dam surface area and catchment volume and its capacity to mitigate flood risks for sustainable development. *Mathematical Modelling of Engineering Problems*, 11(7), 1973–1978.
 22. Ikhsan, M., Anggraini, A., Zahid, M., 2019. Specific gravity and grain size distribution of riverbed sediments: Implications for sediment transport modeling. *Journal of Sedimentary Research*, 89(5), 411–425. <https://doi.org/10.2110/jsr.2019.31>
 23. Kuntjoro, W., Hadi, A.S., Santoso, H., 2017. Evaluation of cross-sectional area and discharge measurements in river hydraulics. *Hydrological Sciences Journal*, 62(4), 592–606. <https://doi.org/10.1080/02626667.2017.1312269>
 24. Maarroof, B.F., Kareem, H.H., 2022. Geomorphometric analysis of Al-Teeb River meanders between Al-Sharhani Basin and Al-Sanaf Marsh, Eastern of Misan Governorate, Iraq. *Misan Journal of Academic Studies (Humanities and Social Sciences)*, 21(42), 441–455.
 25. McCandless, T.L., 2003. *Maryland stream survey: Bankfull discharge and channel characteristics of streams in the coastal plain hydrologic region*. US Fish and Wildlife Service, Chesapeake Bay Field Office, CBFO-S03-02.
 26. Nanson, R.A., Nanson, G.C., Huang, H.Q., 2010. The hydraulic geometry of narrow and deep channels; evidence for flow optimisation and controlled peatland growth. *Geomorphology*, 117(1–2), 143–154.
 27. Odemerho, F.O., 1984. A reduced-rank prediction model of stream-channel size response to traditional agricultural land-use practices in southwestern Nigeria. *Journal of Hydrology*, 70(1–4), 85–100.
 28. Ollero, A., 2010. Channel changes and floodplain management in the meandering middle Ebro River, Spain. *Geomorphology*, 117(3–4), 247–260.
 29. Salahaldain, Z., Naimi, S., Alsultani, R., 2023. Estimation and analysis of building costs using artificial intelligence support vector machine. Available at: <http://dx.doi.org/10.18280/mmep.100203>
 30. Sinnakaudan, S., Van der Laan, M., Klyve, L., 2010. Bed load transport in rivers: The role of sediment size and discharge variations. *River Research and Applications*, 26(5), 559–572. <https://doi.org/10.1002/rra.1268>
 31. Thair, J.M., Imad, A.D., Riyadh, A.A., 2018. Experimental determination and numerical validation of the chloride penetration in cracked hydraulic concrete structures exposed to severe marine environment. In *IOP Conference Series: Materials Science and Engineering*, 454(1), 012099. IOP Publishing.
 32. WRDS (Water Resources Development and Statistics), 2018. *Annual flow and sediment data for Euphrates River: Al-Hilla region*. Iraqi Ministry of Water Resources Report.
 33. Xiaoqing, Y., Yang, X., 2003. *Manual on sediment management and measurement*. Geneva: Secretariat of the World Meteorological Organization, 158.
 34. Forti, L., Pezzotta, A., Zebari, M., Zerboni, A., 2023. Geomorphology of the central Kurdistan Region of Iraq: landscapes of the Erbil Plain between the Great Zab and Little Zab Rivers. *Journal of Maps*, 1–12.